Charge Transfer Study through the Determination of the Ionization Energies of Tetrapeptides X3-Tyr, X = Gly, Ala, or Leu. Influence of the Inclusion of One Glycine in Alanine and Leucine Containing Peptides

Dominique Dehareng* and Georges Dive

Centre d'Ingéniérie des Protéines, Institut de Chimie B6a, Sart Tilman, B4000, Liège, Belgium

Received: July 6, 2006; In Final Form: August 29, 2006

The energies of the fundamental and several excited states of tetrapeptide radical cations were determined at the outer valence Green's function (OVGF) level, at three geometries corresponding to the lowest energy conformations: two for the neutral and one for the cation. The conformations were optimized at the density functional theory level within the B3LYP framework. It was found that, from a purely energetic point of view, a charge initially created on the tyrosine chromophore could migrate without any geometrical change and without further activation once the excited electronic state of the ionized chromophore was formed. This migration could reach the NH_2 terminus for the neutral conformations but should stop at the adjacent peptide link for the cation conformation. These results stress the probable influence of the electronic coupling between the states rather than the existence of a barrier on the charge pathway to explain the difference between the peptides in the charge-transfer process leading to the loss of an iminium $[NH_2{=}CHR]^+$ cation. The dissociation energy of the asymptote related to the formation of this NH_2 terminus iminium cation was calculated for few species and it appears that the excess energy available for dissociation is significant when starting from the lowest energy conformations of the neutral or the cation, provided that the charge transfer is effective. It was also found that the amino acids did not conserve their energetic properties and their zero order energy levels turned to a complete new energetic scheme corresponding to the conformation of the peptide.

Introduction

Charge migration in biological macromolecules is a fundamental widespread process. In protein environments, it is known to be very efficient[1] and is considered as a prototype for distal chemical reactions.[2−4] The model introduced was a bifunctional model:[5] the charge transport along a polypeptide chain involves essential large amplitude chain motions and can be depicted as a virtual particle moving inside the bottom of a Ramachandran plot. The polypeptide is locally ionized and excited at a specific site, either at a carbamide link from which the energy is propagated in the case of molecular dynamics (MD) simulations,[1,5,9] or at a chromophore (a tyrosine, a phenylalanine or a tryptophane) in laser-induced dissociation experiments.[6−8,10]

In the first case concerning MD calculations, energy conservation is observed, which ensures, at long distance, movement of the charge and energy and hence provides a model for chemical reaction at a distance. Each amino acid has a C_α atom acting as a hinge between the amino acids. At each hinge there are two torsional angles, $\phi_{i-1,i}$ and $\Psi_{i,i+1}$. The charge is initially injected into a carbamide group, and its energy is transferred to the two torsional degrees of freedom of the hinge. At the same time this charge is waiting in carbamide$_i$ until the carbamide$_{i+1}$ rotates to a certain angle and distance. Then the charge is transferred with zero activation energy. The electronic transition rate, hopping between two nearby critical structures, lies on the time scale of electronic correlation—i.e., it turns into one hybridized state. In this mechanism the charge is initially excited to an electronic excited state and the excess energy is then carried by the charge. When it moves to an adjacent carbamide group, the charge dumps part of its energy into the torsional degrees of freedom of the next carbamide group because of energy conservation. The torsional period on the hinge is about 150 fs. The MD simulation shows that the motion inside the phase space is stochastic rather than coherent. This process will iterate until the charge reaches the terminal where a chemical reaction occurs (dissociation in the studied cases). Charge transfer was studied on small peptide cations in gas phase[2,3,5−10] as well as in the solvent.[4] The original mechanism survives entering the liquid phase but the effect of the water is to create a hydrophobic jacket around the peptide that seriously constrains the motion of the peptide. Such motion in the peptide is an essential element in the bifunctional model.

As to the gas-phase experiments by Weinkauf et al.,[6−8] the one-color (one 260−280 nm excitation wavelength) and two-color (two excitation wavelengths at 260−280 and 520−260 nm) experiments on the photoionization and photodissociation studies of peptides containing C-terminal aromatic amino acids revealed that some of them were subjects to charge transfer (CT) while others were not. A strong evidence emerged for a threshold behavior of the CT process at about 2−2.5 eV. But according to the authors, calculations of the ground state, excited electronic states of peptide ions at a high level of accuracy is very time-consuming. They performed some calculations at the semiempirical MNDO and PM3-CI levels.[7] Most of their discussion was based on the relative energy positions of the ionization levels, considered to be the estimated ionization energies of the isolated amino acids. Furthermore, the authors made the hypothesis that "the ionization potential of the bridge was estimated to be higher than that of the free N-terminal amino

* Corresponding author. Telephone: +32 4 3663499. Fax: +32 4 3663364. E-mail: d.dehareng@ulg.ac.be.

10.1021/jp064255w CCC: $33.50
Published on Web 10/06/2006

group because of the mesomeric stabilization in the peptide chain which tends to charge the nitrogen atom in the bridge more positive therefore increasing local ionization potential there by estimated 0.4 eV". In ref 10, Cui et al. eliminated prompt ionized fragments and investigated slow dissociation processes occurring very near the threshold, i.e., with rate constants on the order of 10^3 s^{-1}. Their study was based on one-color and two-color experiments too. They also observed selective dissociation at the NH_2 terminus. In their one-color experiment, they ionize and excite the peptide Leu-Tyr and $(Leu)_2$-Tyr with a two + one 266 nm (4.66 eV) photon absorption, respectively. In their two-color experiments, they ionize the peptide with a two 266 nm photon absorption and they excite the cation after a period of relaxation (1980 ms) with a one photon aborption of either 280−289 (4.29−4.43 eV) or 579 nm (2.48 eV). They observed near threshold slow dissociations for both one-color (266 nm) and two-color (266 + 579 nm) experiments but not for the other two-color (266 + 280 nm) one. The result of the one-color expriment was surprising because the excess energy (4.66−5.98 eV) is rather high and should correspond to a dissociation rate constant in the nanosecond time scale. Thus, the authors proposed that the observed slow dissociation should be related with a two-photons absorption instead of a three-photons one, leading to a supposed excess energy of about 1.32 eV, to be compared with 1.5 eV for the estimated needed energy. For the two-color experiments with the 579 nm laser, the rate constant was 4.5 times higher than for the one-color experiment but the excess energy (2.14 eV) was somewhat higher too. These near threshold experiments tend to show that a dissociation leading selectively to the NH_2 terminus iminium cation is already possible with an excess energy of 1.32−2.14 eV.

On the basis of both experimental results and the theoretical models, it was postulated that each amino acid in zero-order contributes semi-independently to the potential energy surface (PES) of the whole polypeptide. According to this hypothesis, the PES could be approximated in first order by the values of the ionization energies (IE) of the separate amino acids and the IE of the whole molecule was not directly relevant there. The nature of the involved amino acids could uniquely predict the charge mobility: insert a high IE amino acid results to stop the charge migration at this site. This model thus proposed a hopping mechanism for the charge-transfer process.[7]

The aim of our work was to bring some more information, on a qualitative basis, about the charge transfer occurring in small peptide cations. The choice of tetrapeptides resulted from a compromise between the size of the systems and the CPU time needed to complete the investigation. This article was not aimed at scanning exhaustively the conformational space of the neutral and the cation peptides. The work was intended to shed some light on the influence of conformation on the energy pattern of the radical cation excited states and thus focus on the determination of ionization energies and cation excitation energies as a function of the conformation, based on quantum chemistry calculations, at the Hartree−Fock level,[11−13] for qualitative descriptions of the molecular orbitals (MO), or outer-valence Green's functions (OVGF)[14−20] for semiquantitative determinations of the IE. The work investigates on tetrapeptides constituted with the aliphatic amino acids alanine, glycine and leucine and terminated by a tyrosine. In the following, the amino acids will be represented either by their three-letter or by their one-letter abbreviations: alanine is Ala or A, glycine is Gly or G, leucine is Leu or L and tyrosine is Tyr or Y. The studied peptides are $(Gly)_3$-Tyr, $(Ala)_3$-Tyr, and $(Leu)_3$-Tyr, as well as $[(Ala)_2$-Gly]-Tyr and $[(Leu)_2$-Gly]-Tyr, where the position of Gly is varied along these latter chains.

Section 2 briefly presents the computational tools, and section 3 presents the definition of the ionized states.

Section 4 introduces the results, and section 5 develops the main results into a general discussion.

Computational Tools

All the calculations were performed with the Gaussian 98[21] program on a SGI Origin 3800. All the chosen conformations were fully optimized within the density functional theory (DFT)[22] and the Kohn−Sham molecular orbital formalism,[23] using the hybrid method B3LYP[24] with the 6-31G**(5d)[25,26] basis set. The choice of this calculation level relies on the fact that it constitutes a good compromise between the quality of the results and the size of the studied systems. However, though some studies can show that it provides a good energy ordering of the lowest conformations compared with experimental results,[27] in many cases this is not necessarily true,[28−30] though usually the most stable conformation is correctly assigned. In our previous study on amino acids,[20] it was already shown that B3LYP/6-31G** did not classify the low energy conformations as other correlated methods did (MP2, QCI, CCSD). Nevertheless, since this article is not aimed at finding all the low energy conformations but only to study the conformation influence on the ionization energies, this calculation level was chosen.

The ionization energies were determined with the outer valence Green's function (OVGF) method using the smaller 6-31G basis set, due to the size of the systems. The choice of this method was justified as follows. Time-dependent density functional theory (TDDFT) is increasingly popular for determining excited states energies.[17,31−34] It has been recognized to often provide qualitatively good energy values within a 0.4 eV error range. However, some erroneous results are also known in particular when the system size increases.[35] Nevertheless, this method has the great advantage to be applicable to large systems. As to the OVGF method, it already proved interesting[17−20] as it could often fit with experimental results in a 0.3 eV range. As a previous study of our laboratory on amino acids was already performed at the OVGF level, it was decided to go on with this method as this work is essentially intended to remain at a qualitative or semiquantitative level. The advantage of OVGF is that it provides an easy way to know the character of the ionized state through the shape of the ionized MO, obtained at the RHF level. Its drawback is that it cannot account for the shake-up ionic states, i.e., those states that do not come only from a direct ionization event but that also include electronic excitation. Here follows a brief recall of the method. It is based on the one-particle concept.

The definition of a Green's function[13] is linked to an operator. The operator in our case is obviously the many-body Hamiltonian, be it the real one H or an approximate one H_0. Let Ψ_i and E_i designate the eigenfunctions and eigenvalues of this Hamiltonian. The one-particle Green's function associated with the Hamiltonian is given by the expression

$$G(r,r',E) = \sum_i (\Psi_i(r)\ \Psi_i^*(r'))/(E - E_i),$$

with E being a parameter.

It is usually its matrix representation that is considered in quantum chemistry, and its elements are calculated with the Ψ_i as basis functions. In the specific case of the Hartree−Fock framework, one can define the zero-order, or approximate,

Hamiltonian as the sum of the Fock operators, $H_0 = \Sigma_i F(i)$, for which the associated Green's matrix is given by

$$\mathbf{G}_0(E) = (E\,\mathbf{1} - \epsilon)^{-1}$$

1 being the unity matrix and ϵ the diagonal matrix the elements of which are the MO energies. When the parameter E varies, the elements of G_0 can become infinite; i.e., they have a pole, at the values corresponding to the MO energies.

For a real Hamiltonian expressed as $\mathbf{H} = \mathbf{H}_0 + \mathbf{V}$, the Green's matrix is given by

$$\mathbf{G}(E) = (E\,\mathbf{1} - \mathbf{H}_0 - \mathbf{V})^{-1}$$

and obey the equation

$$\mathbf{G}(\mathrm{E}) = \mathbf{G}_0(\mathrm{E}) + \mathbf{G}_0(\mathrm{E})\,\mathbf{V}\,\mathbf{G}(\mathrm{E})$$

As a matter of fact, the ϵ_i are approximations of differences between Hamiltonian eigenvalues of the neutral and of the ionized molecule (Koopmans' theorem). Thus, we should try to obtain a $G(E)$ with poles at the exact energy differences between the N and the $N - 1$ particle systems and be able to improve upon Koopmans' theorem while retaining the one-particle picture associated with HF. However, to account for the two-particle characteristics of the real Hamiltonian, Dyson[13] introduced an effective energy dependent potential, $\Sigma(E)$, named the self-energy, to replace **V**: $\mathbf{G}(E) = \mathbf{G}_0(E) + \mathbf{G}_0(E)\,\Sigma(E)\,\mathbf{G}(E)$, which can be rewritten as

$$\mathbf{G}(E) = (E\,\mathbf{1} - \epsilon - \Sigma(E))^{-1}$$

The improvement upon the Koopman's theorem comes from the evaluation of the self-energy matrix. It is expressed within the perturbation framework as a sum of different order terms that are evaluated as functions of the field operators (creation and annihilation operators and their products). This matrix takes into account the relaxation and the correlation effects upon ionization. It is expressed as a function of the bielectronic integrals in the MO basis and its terms have denominators of the type $(E - \epsilon_i - \epsilon_j - \epsilon_a - \epsilon_b)$. The ionization energies are found iteratively through a scan of the E parameter, to find the poles of the matrix $\mathbf{G}(E)$. At the OVGF level, the self-energy matrix is considered diagonal and its elements are expanded to the third order of perturbation.

The MOs taken into account in this method were all the occupied valence ones augmented by the same number of virtual MOs. In the case of $(Leu)_3$-Tyr and $[(Leu)_2$-Gly]-Tyr, this MO number was too large to be tractable and it was reduced in the following way. The number of occupied valence MOs did no longer include the MOs corresponding to the main occupation of the oxygen and nitrogen 2s basis functions in all these cases. For the $[(Leu)_2$-Gly]-Tyr isomers, the number of virtual MOs was reduced to the set corresponding to orbital energies equal or below 0.7 au (instead of ~0.85), and for $(Leu)_3$-Tyr, this set was further reduced to energies below or equal to 0.5 au.

Two electronic excited-state geometries were optimized for the $(Leu)_3$-Tyr^+ cation at the UB3LYP level. Though the DFT provides a well-defined framework for the electronic fundamental state through the Hohenberg−Kohn theorem, the way the MOs are derived via the Kohn−Sham formalism can provide excited-state densities, just as UHF does. These excited-state densities or MOs are extrema for the Kohn−Sham equations but not minima since a slight deviation from their converged shape makes them drop down to the fundamental state functions, process known as the variational collapse in HF. In practice, it is possible to obtain the electronic excited state MOs only in a few happy cases and it is much easier in the UHF framework than in the UB3LYP one. Thus, the UHF MOs were first derived with the 6-31G basis set to obtain a good guess and then the UB3LYP/6-31G** MOs were calculated and the geometry optimization was performed.

CHART 1

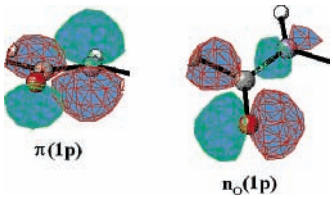

Dissociation energies related to the formation of the terminus $[NH_2{=}CHR]^+$ iminium cation were calculated at the UB3LYP/6-31G** level for aliphatic dipeptide cations. Three other dissociation channels were also considered for $(Ala)_2^+$. These energies (ΔE_{diss}) were calculated as the difference between the energy of the optimized geometry of the dissociating excited state, already bearing the charge on the NH_2 terminus, and the energy of the fragments.

Description of the Ionized States

The ionized states studied in this work correspond to direct ionization of the MOs with no further electronic excitation; i.e., no shake-up states will be mentioned though they are known to play important roles in the coupling between excited states and thus in electron-transfer processes. All the states will be referred to by the label of their related ionized MO, i.e., the π1(Y) (see below) state results from the ionization of the π1 MO localized on the tyrosine ring. Most of the MOs have been found to be highly or moderately localized on one part of the polypeptide and will be labeled according to the nuclei on which they are mainly centered. The degree of localization and thus the way the MOs are labeled is based on 3D contour plots drawn at 0.05 au by the program Gaussview.[36] On the peptide link, the MOs that are the highest in energy, i.e., the most easily ionizable, are of two types: π-type because the MO density presents a nodal plane passing through the backbone nuclei, and an oxygen lone-pair-type very often mixed with some σ-type density on one of the adjacent C−C bonds. These two types of MO will be labeled as $\pi(i\mathrm{p})$ and $n_O(i\mathrm{p})$ respectively, with the number i of the related peptide link in parentheses as presented in Chart 1. The NH_2 and COOH termini are also characterized by lone pair and π-type MO densities corresponding to the lone pairs on either the nitrogen or the carbonyl oxygen on one hand, and to a density presenting a nodal plane passing through the COOH nuclei on the other hand. The lone-pair types on the oxygen will be denoted n(tO═C) and the other two will be labeled n(Nt) and π(COOH); they are presented in Chart 2. In the n(tO═C) MO, the carbonyl oxygen lone pair can be mixed with a small density part from the OH oxygen, and it also shows a density on the $\sigma(C_\alpha{-}C)$. The three π densities on the tyrosine ring will be denoted, respectively, as π1(Y), π2(Y), and π3(Y); they are much alike those obtained for the phenol, as seen in Chart 3.

Some MO densities are localized on the σ bonds of either the tyrosine ring or of the C−C of C−H skeleton between the C_α and the C_γ; these are respectively denoted as σ's(Y) and σ's(sdY). Moreover, for the peptides containing leucine, several σ-type MOs are localized on the C−C and C−H skeleton of

CHART 2

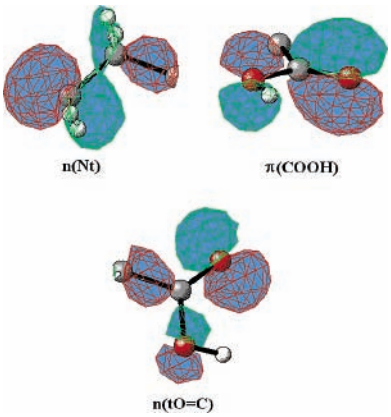

CHART 3

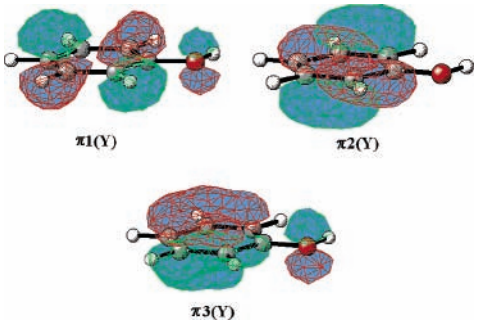

CHART 4

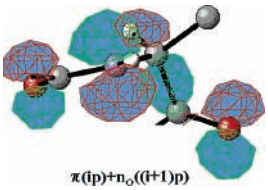

the Leu side chain and they are labeled by Sdch(Li), i being the position of the leucine. In some cases, when the MO shows a delocalized character, the MO density contours at 0.05 au present numerous very small volumes on the skeleton which are specified in square brackets [] in the tables. In Chart 4 is also shown a density for a [$\pi(ip) + n_O((i+1)p)$] MO.

Conformations Building. Some small di- or tripeptides were already studied experimentally and theoretically.[27−30,37−39] From these studies, it appears that several conformations are observable experimentally; i.e., there exist several low-lying conformations that are very close to one another. To our knowledge, no theoretical studies exist on tetrapeptides.

The initial conformations of the neutral tetrapeptides were constructed in a stepwise manner, on the basis of alanine peptides. It was started with the dipeptide Ala-Tyr at the B3LYP/6-31G level. Seven conformations characterized by different intramolecular interactions were hand-built using the Gaussview program.[36] The following observations were used to build the tripeptide $(Ala)_2$-Tyr. The terminus NH_2 adopted the preferred orientation with its nitrogen pointing toward the H−N of the next residue, instead of having its hydrogens interacting with the O═C of the first residue. The COOH terminus liked interacting with either the H−N in the last residue or the O═C of the previous one. In the construction of the tripeptide, followed by the tetrapeptide, the intramolecular interactions leading to preferred conformations were considered finally leading to 11 conformations for $(Ala)_3$-Tyr. The side chain was then adapted to either $(Gly)_3$-Tyr or $(Leu)_3$-Tyr by using Gaussview. The procedure just described to generate the conformations clearly does not cover the whole conformational space, and it cannot be stated that we obtained the lowest lying conformations.

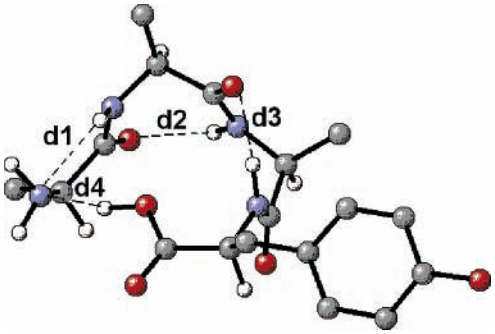

Figure 1. Lowest energy conformation CF1 for the three neutral species X_3-Tyr, X = Gly, Ala, and Leu. Only the backbone hydrogens (white) and only the C_β of the X = Ala or Leu side chains are shown. The carbons, nitrogens and oxygens are respectively shown in gray, blue, and red.

TABLE 1: Intramolecular Distances (Å) Found in CF1 As Shown in Figure 1

peptide	d1	d2	d3	d4
$(Gly)_3$-Tyr	2.337	2.172	2.093	1.815
$(Ala)_3$-Tyr	2.306	2.125	1.971	1.863
$(Leu)_3$-Tyr	2.304	2.143	1.971	1.861
Gly-$(Ala)_2$-Tyr	2.343	2.166	1.972	1.812
Ala-Gly-Ala-Tyr	2.306	2.139	1.975	1.863
$(Ala)_2$-Gly-Tyr	2.294	2.151	2.090	1.812
Gly-$(Leu)_2$-Tyr	2.350	2.188	1.972	1.813
Leu-Gly-Leu-Tyr	2.300	2.132	1.969	1.872
$(Leu)_2$-Gly-Tyr	2.286	2.170	2.083	1.806

For the cation conformations, a first step was conducted on the $(Ala)_3$-Tyr^+ cation; it was started from the optimized geometries of the 11 neutral conformations of $(Ala)_3$-Tyr. Since most of the cation conformations were much higher in energy than the most stable one, only three or four conformations were optimized for the $(Gly)_3$-Tyr^+ and $(Leu)_3$-Tyr^+ cations, based on the lowest energy conformations of $(Ala)_3$-Tyr^+. It will be shown below that only one or two conformations are low in energy.

Results

A. Comparison between $(Gly)_3$-Tyr, $(Ala)_3$-Tyr and $(Leu)_3$-Tyr (X_3-Tyr). *A.1. Geometry and Relative Energies of the Neutrals.* Among all the 11 conformations searched for the neutral of the X_3-Tyr peptides, the lowest energy structure, denoted CF1, is the same for the three species. It is characterized by four intramolecular backbone interactions (see Table 1 and Figure 1).

The relative energies of the other conformations can be very different according to X. For instance, the number of conformations lying in the range of 15 kJ/mol above the CF1 energy is equal to 3, 5, and 5 for X = Gly, Ala, and Leu, respectively. The conformations are denoted CF*i* with *i* increasing like the relative energies found in $(Ala)_3$-Tyr. The whole set of conformations is presented in Figure 2. The structurally related conformations of the other peptides are not necessarily ordered the same way according to their relative energies, and Table 2 presents both the relative energies and their position number according to the energy scale. It must be pointed out here that a systematic search for the different conformations related to the Leu side chains was not performed in this study. It appears

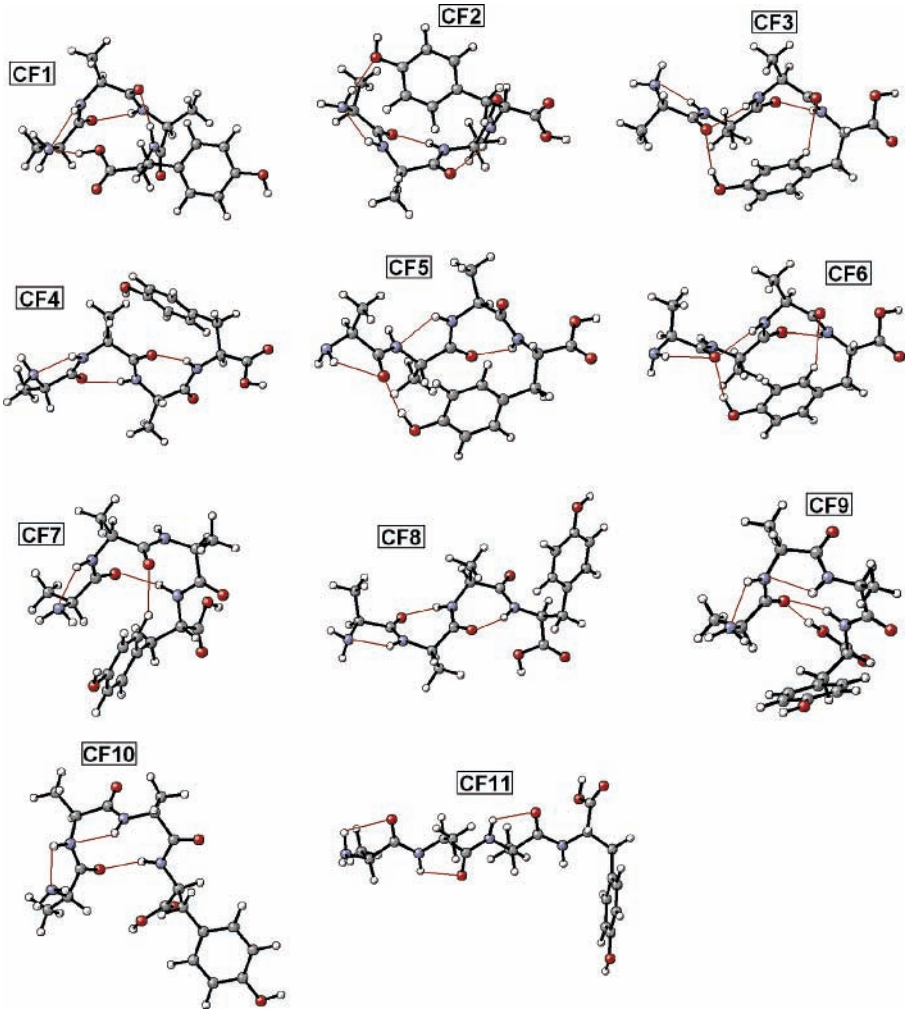

Figure 2. Eleven optimized conformations for the neutral $(Ala)_3$-Tyr tetrapeptide. The intramolecular interactions are shown in brown.

TABLE 2: Relative Energies (kJ/mol) for the Five Lowest Energy Conformations[a]

peptide	CF1	CF2	CF3	CF4	CF5
(Gly)3-Tyr	0.0	6.52 (2)	13.32 (3)	18.69 (4)	26.04 (7)
(Ala)3-Tyr	0.0	0.97 (2)	3.30 (3)	7.87 (4)	14.56 (5)
(Leu)3-Tyr	0.0	0.24 (2)	12.94 (5)	6.50 (3)	8.64 (4)
Gly-$(Ala)_2$-Tyr	0.0	3.37 (2)	5.47 (3)	10.41 (4)	15.41 (5)
Ala-Gly-Ala-Tyr	6.64 (2)	0.0	7.23 (3)	10.92 (4)	19.20 (5)
$(Ala)_2$-Gly-Tyr	0.0	15.21 (2)	18.11 (3)	22.35 (4)	30.94 (5)
Gly-$(Leu)_2$-Tyr	0.0	3.80 (2)	14.11 (5)	9.95 (3)	11.67 (4)
Leu-Gly-Leu-Tyr	6.05 (3)	0.0	4.89 (2)	not found	17.41 (4)
$(Leu)_2$-Gly-Tyr	0.0	15.84 (2)	29.21 (6)	23.67 (3)	26.08 (5)

[a] In parentheses is given the number of the conformation according to its relative energy scale position.

that CF1 is certainly the most populated conformation for $(Gly)_3$-Tyr but that CF2 is nearly degenerate with CF1 for $(Ala)_3$-Tyr and $(Leu)_3$-Tyr. In the case of $(Ala)_3$-Tyr, CF3 could also be represented in the whole population of conformations.

A.2. Geometry and Relative Energies of the Cations. The lowest energy conformation obtained came from the ionization of CF3, and in fact, two slightly different conformations were obtained, in the range of 3.10 kJ/mol, and denoted CF1c and CF2c, as presented in Figure 3. The third lowest energy cation conformation lies at 24.80 kJ/mol above CF1c. From the results obtained for $(Ala)_3$-Tyr^+, several cation conformations were also optimized for $(Gly)_3$-Tyr^+ and $(Leu)_3$-Tyr^+, and the lowest energy conformation obtained was also CF1c with similar gaps (around 18 kJ/mol) for the third and higher states.

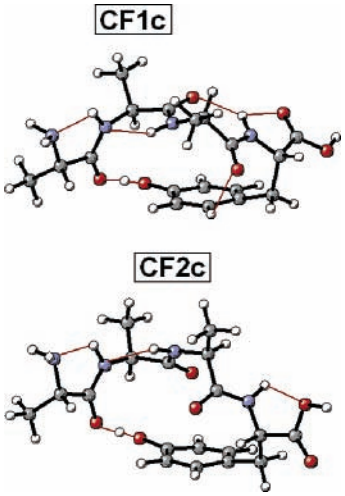

Figure 3. Two similar lowest energy optimized conformations of the radical cation $(Ala)_3$-Tyr^+.

For the $(Leu)_3$-Tyr^+ cation, a geometry optimization of the two $[\pi(1p) + n_O(2p)]$ and $[n(Nt) + n_O(1p)]$ excited states was performed at the UB3LYP/6-31G** level with CF1 as starting geometry. The only excited states obtainable with this method were those above-mentioned. From the optimized geometrical structures, shown in Figure 4, it is obvious that the optimized geometry can vary significantly as a function of the charge localization, though they were all generated starting from CF1 (as denoted in the figure by > CF1).

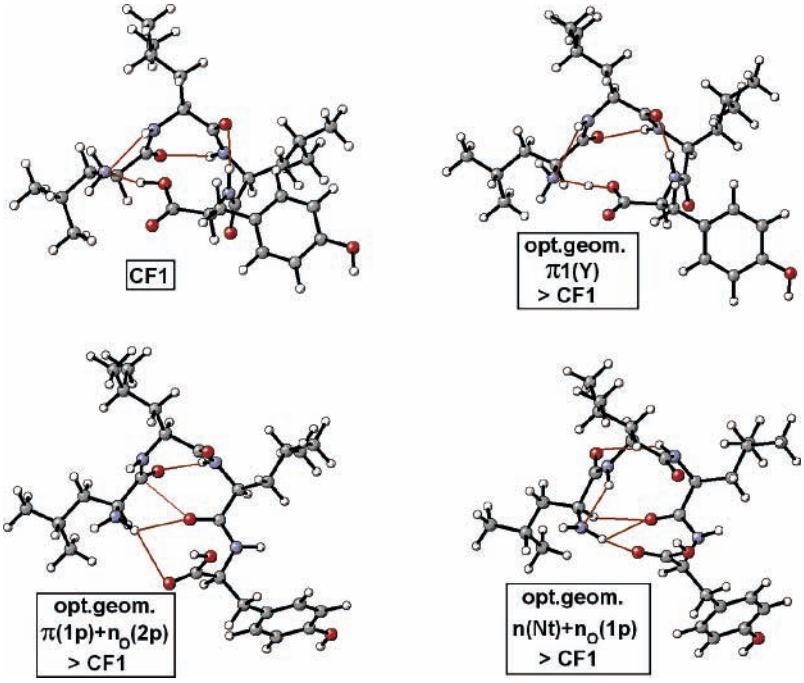

Figure 4. Optimized geometries of $(Leu)_3$-Tyr: the lowest energy conformation of the neutral CF1, the conformation of the fundamental electronic state $\pi 1(Y)$ of the cation starting from CF1 (denoted >CF1), and the conformations of two excited states $[\pi(1p) + n_O(2p)]$, $[n(Nt) + n_O(1p)]$ of the cation starting from CF1 (denoted >CF1).

A.3. Ionization Energies. The ionization energies were determined for three geometries, CF1, CF2, and CF1c, and are presented in Table 3.

The choice of these conformations is justified by the following. The determination of vertical ionization energies implies that the calculation is made on the most stable conformation of the neutral, i.e., CF1. Since CF2 is very close to CF1, it can be supposed that this conformation will also be present in the population of the neutral. As to the choice of the most stable cation conformation CF1c, it was also chosen in order to determine excitation energies for the cation in its relaxed geometry, since some experiments may lead to such species. As a matter of fact, a vertical ionization energy is not interesting at this geometry, even if it will be given in the tables, since the neutral species will not adopt such a distorted geometry and thus experimentally it will not be seen.

The size of the side chain acts differently according to the conformation: on CF1 and CF1c, the low ionization energies tend to decrease as the size increases, but this is not a generality for CF2.

The $\pi 1(Y)$, $\pi(3p)$, $\pi(2p)$, and $\pi(1p)$ states are always found in this order within the five first ionized levels according to their energy, with the exception of CF2 for $(Ala)_3$-Tyr and $(Leu)_3$-Tyr where $\pi(3p)$ and $\pi(2p)$ have switched but are very close ($\Delta E = 0.02$ and 0.13 eV respectively). Furthermore, according to the RHF MO corresponding to the ionization event, $\pi(2p)$ and $\pi(1p)$ are always mixed with the oxygen lone pair of the following peptide link, i.e., $n_O(3p)$ and $n_O(2p)$, respectively. The other combinations $n_O(3p) + \pi(2p)$ and $n_O(2p) + \pi(1p)$ are found higher in energy. As to the state corresponding to the ionization of $\pi 2(Y)$, it is always the second state found in the cation conformation CF1c, i.e., found between $\pi 1(Y)$ and $\pi(3p)$, but it lies higher than $\pi(3p)$ or even $\pi(2p)$ for the conformations of the neutral, except in the case of the CF1 for $(Gly)_3$-Tyr and $(Leu)_3$-Tyr where the $\pi 2(Y)$ and $\pi(3p)$ states are nevertheless very close, quasi degenerate.

Excitation energies of the cations (ΔE_{exc}) are also provided in Table 3 and are defined as the energies of the considered state by reference to the fundamental cationic state (which is always the $\pi 1(Y)$ state). Let us focus on three excited states: $\pi(3p)$, n(Nt), and $\pi 3(Y)$. The first state is interesting because it corresponds to the localization of the charge on the ionizable group just next to the initial localization on the tyrosine. The second state interest comes from the fact that the observed charge transfer finally leads to this state since the mass spectra show a preference for the formation of iminium ion $[NH_2{=}CHR]^+$ (R being the side chain) when charge migration occurs. And finally, the interest of $\pi 3(Y)$ is to be the initial photoexcitable state prior to charge transfer and eventual dissociation.

The excitation energy of the $\pi(3p)$ and n(Nt) states largely depends on the conformation (from 0.6 to 2.4 eV for $\pi(3p)$ and from 1.1 to 4.4 for n(Nt)) and much less on the nature of the side chain (G, A, L). The same remark stands for both $\pi(2p)$ and $\pi(1p)$. This is not the case of $\pi 3(Y)$ which scans a much smaller energy range (from 3.4 to 3.8 eV). The lowest excitation energy for $\pi(3p)$ is 0.57, 0.57, and 0.69 eV, found for CF2 (G, A, L) while it grows up to 1.06, 0.86, and 1.15 eV for CF1 and even much higher for CF1c: 2.24, 2.26, and 2.40 eV. The same trend (lowest ΔE_{exc} for CF2, highest for CF1c) is found for n(Nt), as well as for $\pi(2p)$ and $\pi(1p)$. The $\pi 2(Y)$ presents an intermediate behavior since its ΔE_{exc} does not vary much between the neutral conformations, in the [0.82−0.95 eV] range, but it changes significantly for the cation conformation CF1c with a ΔE_{exc} around 1.65 eV. Thus, the relative position of the $\pi 2(Y)$ state as compared to the $\pi(ip)$ states varies from one conformation to the other. From the description of the ionized MO, the n(Nt) state for CF1c seems to present a delocalized charge in the three peptide cations while this charge is much more localized on the NH_2 terminus with a partial delocalization on the oxygen of the first peptide link for the neutral conformations. Similarly, while the $\pi 3(Y)$ state tends to show a well-localized $\pi 3$ ionized MO, it nevertheless presents a more delocalized MO for CF1 of $(Ala)_3$-Tyr and $(Leu)_3$-Tyr. For all the neutral conformations studied, the n(Nt) state is always lower in energy than the $\pi 3(Y)$ state but higher than each $\pi(ip)$ state,

TABLE 3: Ionization Energies (IE) and Cation Excitation Energies (ΔE_{exc}) Calculated at the OVGF/6-31G Level for Three Conformations of (Gly)3-Tyr, (Ala)3-Tyr, and (Leu)3-Tyr[a]

CF1		CF2		CF1c	
MO description	IE (eV)/ΔE_{exc}	MO description	IE (eV)/ΔE_{exc}	MO description	IE (eV)/ΔE_{exc}
		$(Gly)_3$-Tyr			
π1(Y)	7.80/0.0	π1(Y)	8.13/0.0	π1(Y)	6.33/0.0
π2(Y)	8.74/0.94	π(3p)	8.70/0.57	π2(Y)	7.99/1.66
π(3p)	8.86/1.06	π(2p) + n_O(3p)	8.79/0.66	π(3p)	8.57/2.24
π(2p) + n_O(3p)	9.03/1.23	π2(Y)	8.97/0.84	π(2p) + n_O(3p)	8.95/2.62
π(1p) + n_O(2p)	9.48/1.68	π(1p) + n_O(2p)	9.14/1.01	π(1p) + n_O(2p)	9.70/3.37
n(Nt) + n_O(1p)	10.34/2.54	n(Nt) + n_O(1p)	9.42/1.29	σ's(Y) + n_O(1p)	9.91/3.58
n_O(3p) + π(2p)	10.44/2.64	n_O(3p) + π(2p)	10.20/2.07	π3(Y)	10.05/3.72
n_O(2p) + π(1p)	10.78/2.98	n_O(2p) + π(1p)	10.50/2.37	n_O(3p) + π(2p)	10.26/3.93
n(tO═C) + n_O(2p) + n_O(1p)	10.85/3.05	n(tO═C) + n_O(1p) + n(Nt)	10.88/2.75	n(tO═C)	10.48/4.15
π3(Y) + n(tO═C)	11.23/3.43	n_O(1p) +n(Nt) + n(tO═C)	10.93/2.80	n(Nt) + n_O(1p) + n(tO═C)	10.69/4.36
n(Nt) + n_O(1p) + π(COOH)	11.24/3.44	π(COOH)	11.51/3.38	σ's(Y) + σ's(sdY) + n(tO═C)	11.04/4.71
σ's(Y) + π(COOH)	11.52/3.72	π3(Y)	11.57/3.44	n_O(2p) + π(1p)	11.16/4.83
σ's(Y) + π(COOH)	11.62/3.82	σ's(Y)	11.90/3.77	π(COOH)	11.62/5.29
				n(Nt) + n_O(1p) + σ's(Y)	11.52/5.19
		$(Ala)_3$-Tyr			
π1(Y)	7.72/0.0	π1(Y)	8.05/0.0	π1(Y)	6.25/0.0
π(3p)	8.58/0.86	π(2p) + n_O(3p)	8.60/0.55	π2(Y)	7.92/1.67
π2(Y)	8.64/0.92	π(3p)	8.62/0.57	π(3p)	8.51/2.26
π(2p) + n_O(3p)	8.80/1.08	π2(Y)	8.88/0.83	π(2p) + n_O(3p)	8.81/2.56
π(1p) + n_O(2p)	9.21/1.49	π(1p) + n_O(2p)	8.96/0.91	π(1p) + n_O(2p)	9.45/3.20
n(Nt) + n_O(1p)	10.06/2.34	n(Nt) + n_O(1p)	9.25/1.20	σ's(Y) + n_O(1p)	9.75/3.50
n_O(3p) + π(2 p)	10.13/2.41	n_O(3p) + π(2p)	10.03/1.98	π3(Y)	9.96/3.71
n_O(2p) + π(1p)	10.50/2.78	n_O(2p) + π(1p)	10.20/2.15	n_O(3p) + π(2p)	10.13/3.88
n(tO═C) + n_O(1p) [+n_O(3p)]	10.64/2.92	n_O(1p) + n(Nt)	10.52/2.47	n(Nt) + n_O(3p) + n(tO═C)	10.36/4.11
π(COOH)[+π3(Y)]	11.10/3.38	n(tO═C)	10.91/2.86	n(tO═C) + n(Nt)	10.55/4.30
n(Nt) + π3(Y) + π(COOH)	11.14/3.42	π(COOH)	11.47/3.42	n_O(2p) + π(1p) +σ's(sdY)	10.85/4.60
n(Nt) + n(tO═C) + π3(Y)	11.17/3.45	π3(Y)	11.49/3.44	n_O(2p) + π(1p) +σ's(sdY)	11.07/4.82
σ's(Y)	11.60/3.88	σ's(Y)	11.84/3.79	n_O(1p) + n(Nt) +σ's(Y)	11.33/5.08
				π(COOH)	11.61/5.36
		$(Leu)_3$-Tyr			
π1(Y)	7.69/0.0	π1(Y)	8.04/0.0	π1(Y)	6.17/0.0
π2(Y)	8.58/0.89	π(2p) + n_O(3p)	8.60/0.56	π2(Y)	7.83/1.66
π(3p)	8.64/0.95	π(3p)	8.73/0.69	π(3p)	8.57/2.40
π(2p) + n_O(3p)	8.80/1.11	π2(Y)	8.86/0.82	π(2p) + n_O(3p)	8.78/2.61
π(1p) + n_O(2p)	9.14/1.45	π(1p) + n_O(2p)	8.88/0.84	π(1p) + n_O(2p)	9.31/3.14
n(Nt) + n_O(1p)	9.91/2.22	n(Nt) + n_O(1p)	9.14/1.10	n_O(1p) + n(Nt) + σ's(Y)	9.67/3.50
n_O(3p) + π(2p)	10.17/2.48	n_O(3p) + π(2p)	10.03/7.01	π3(Y)	9.93/3.76
n_O(2p) + π(1p)	10.44/2.75	n_O(2p) + π(1p)	10.18/2.14	π(2p) + n_O(3p)	10.06/3.89
n_O(tO═C) + n_O(1p) + n(Nt)	10.66/2.97	n(Nt) + n_O(1p)	10.52/2.48	n(Nt) [+n_O(3p) + σ's(Y)]	10.27/4.10
π(COOH) +Sdch(L3)	11.16/3.47	Sdch(L3)	11.05/3.01	n_O(tO═C)	10.60/4.43
Sdch(L3) + n_O(tO═C) + n(Nt)	11.17/3.48	Sdch(L3)	11.08/3.04	π(1p) + n_O(2p)	10.69/4.52
Sdch(L3)	11.29/2.60	Sdch(L3)	11.09/3.05	Sdch(L,Y)	11.26/5.09
π3(Y) +Sdch(L3)	11.31/3.62	n(tO═C)	11.15/3.11		
π(COOH) +Sdch(L3)	11.32/3.63	Sdch(L2)	11.50/3.46		
Sdch(L3) + n_O(tO═C) + Sdch(L2)	11.43/3.74	Sdch(L1−2) + π(COOH)	11.52/3.48		
Sdch(L2)	11.53/3.84	Sdch(L1−2)	11.55/3.51		
		π3(Y)	11.55/3.51		
		Sdch(L1)	11.59/3.55		
		π(COOH)	11.63/3.59		

[a] The description of the ionized MOs is based on a RHF calculation.

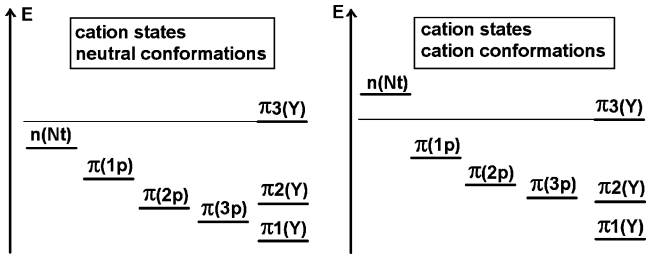

Figure 5. General sketch of the cation energy levels found for the neutral and in the cation conformations.

as presented schematically in Figure 5. This is not the case for the cation conformation CF1c except for $(Leu)_3$-Tyr. Let us emphasize that the π3(Y) state is nearly degenerate with a state that should present a charge on NH_2 for CF1 of $(Gly)_3$-Tyr and $(Leu)_3$-Tyr and that it presents itself a delocalization on NH_2 for CF1 of $(Ala)_3$-Tyr. No such degeneracy or delocalized character is found for CF2 or CF1c.

A comparison with ionization energies obtained at the UHF/6-31G level is performed for the three conformers of $(Leu)_3$-Tyr, to check the atomic spin densities of the ionized state and be sure of the qualitative description obtained by the OVGF/RHF(MO) method. All the ionized states could not be obtained due to variational collapse of the guess onto a lowest state. All the obtained cation states are presented in Table 4. Because of the size of the basis set and the low level of the calculation (UHF is not recommended for ionization energies), the excitation energies are not correlated with the results in OVGF. One interesting point to emphasize it that, according to the atomic spin densities, the description of the mixed character of the

TABLE 4: Excitation Energies ΔE_{exc} (eV) Calculated at the UHF/6-31G Level for the Three Conformations of (Leu)$_3$−Tyr[a]

CF1		CF2		CF1c	
state	ΔE_{exc}(eV)	state	ΔE_{exc}(eV)	state	ΔE_{exc}(eV)
π1(Y)	0.0	π1(Y)	0.0	π1(Y)	0.0
π(3p)	0.35	n_O(3p)	0.17	π2(Y)	1.82
π(2p)	0.83	π(2p)	0.27	π(3p)	1.94
π(1p)	1.19	π(1p)	0.59	n_O(2p)	2.75
n_O(1p)	1.37	π2(Y)	0.69	π(2p) + n_O(3p)	3.14
		n(Nt)	1.07	n_O(1p)	3.51
		Sdch(L3)	3.27	n(Nt) + n_O(1p)	4.55

[a] The description of the state is based on the atomic spin densities.

SCHEME 1

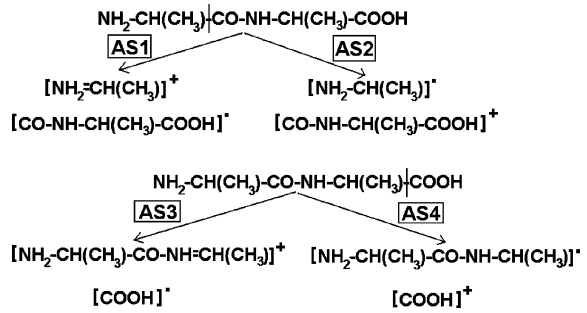

π(2p) + n_O(3p) and n(Nt) + n_O(1p) states is found only for CF1c, the π(*i*p), n_O(*i*p), and n(Nt) spin densities being much more localized for the neutral conformations. At the UHF level, only the reorganization of the electronic cloud is taken into account in the ionization event but the consideration of electronic correlation through post-HF calculations usually provide more delocalized descriptions. Obviously, the two nearly degenerate n_O(3p) and π(2p) states obtained for CF2 should become linear combinations with larger energy gap in between. The trend of π2(Y) to be higher than one or two π(*i*p) for the neutral CF2 conformation but not for the cation one is also found at this level. Similarly, the interesting characteristics of low-lying and energetically different π(*i*p) states is confirmed. The general tendency that the IE are lower for CF2 and higher for CF1c is also confirmed.

A.4. Dissociation Energy for the Iminium Cation Formation. Due to the size of the tetrapeptides, the evaluation of the energy needed to dissociate the cation into its terminal iminium cation and its counterpart was conducted on smaller models and it was chosen to consider some dipeptides.

Four dissociation channels were studied for the L-alanyl-L-alanine cation $(Ala)_2^+$, as presented in Scheme 1. The levels associated with the asymptotes are denoted AS*i*, $i = 1, 4$. Two conformers were optimized for $[CO-Ala]^x$, $x = 0, +1$, and for $[Ala\text{-}CO-NH-CHCH_3]^x$. The lowest energy conformations were considered for the determination of the asymptote relative energies. The lowest energy asymptote is AS1. The energy levels ΔE(AS*i*) of the AS*i* by reference to AS1 are the following: ΔE(AS2) = 1.17 eV, ΔE(AS3) = 0.56 eV, and ΔE(AS4) = 2.87 eV, which shows that the dissociation energies leading to AS1 and AS3 are the closest. Only the AS1 dissociation channel is considered below.

To assess the influence of the side chain on the dissociation energy, its determination was performed for $(Gly)_2$, $(Ala)_2$, $(Leu)_2$, Gly-Ala, and Ala-Gly. The dissociation energy was calculated by reference to the optimized electronic state characterized by a large atomic spin density on the NH_2 terminus, i.e., the n(Nt) state. Two conformations were also considered for the dipeptide cations as well as for the [CO−NH−CHR−COOH] radical. The dissociation energies corresponding to the lowest energy conformers are presented in Table 5, with or without the zero point energy (ZPE) correction.

The dissociation energy from Gly-X and leading to the smallest iminium ion $NH_2{=}CH_2^+$ is always significantly larger (about 0.5 eV) than the other ones. This could have an incidence in the Gly-X_2-Tyr$^+$ cations. The ZPE is not very important, on the order of 0.05−0.08 eV. The ΔE_{diss} decreases from $(Gly)_2^+$ to $(Leu)_2^+$.

However, the value calculated for (Leu)$_3$-Tyr$^+$ is much larger than those obtained for the dipeptides. This can be due to several reasons. The first one is that only one conformer of the parent ion and the fragments was optimized. A second one is that the parent ion is more stabilized by the whole molecular skeleton than the dipeptide cations. This can be pointed out by the bond length between the Cα of the first residue and the C=O, i.e., the scissile bond. In the dipeptide cations, it is equal to 1.6811, 1.7248, and 1.7292 Å for $(Gly)_2^+$[n(Nt)], $(Ala)_2^+$[n(Nt)], and $(Leu)_2^+$[n(Nt)], respectively, and to 1.6307 Å in (Leu)$_3$-Tyr$^+$[n(Nt)].

Nevertheless, the n(Nt) state formed during the experiments is not necessarily in its optimized geometry. Thus, the determination of the energy differences between the asymptote level AS1 corresponding to the iminium $[NH_2{=}CHR]^+$ formation and several other reference energies was performed, as schematized in Figure 6. The ΔE_{diss}() in Table 5 refer to the optimized geometry of the cation in its n(Nt) state, with or without the zero point energy ZPE correction. The ΔE_{AS1}(CF1/n(Nt)) (ΔE_{AS1}(CF1/π3(Y))) and ΔE_{AS1}(CF2/n(Nt)) (ΔE_{AS1}(CF2/π3(Y))) correspond to dissociation energies calculated with reference energies obtained by adding the ionization energy necessary to form the n(Nt) (π3(Y)) state to the energy of the neutral, either CF1 or CF2. For ΔE_{AS1}(CF1c,π3(Y)), the reference energy is obtained by adding the excitation energy of the π3(Y) state to the energy of the cation in its CF1c geometry. A negative ΔE_{AS1} energy means that the parent cation formed has an excess energy relative to the dissociation asymptote. If this excess is small, the dissociation will be slow and vice versa, not taking into account the CT process necessary to form the n(Nt) state. From the results in Table 5, the n(Nt) state produced from the CF2 neutral is the only one to be unable to reach dissociation. Nevertheless, the asymptote can always be reached when the cation keeps the excess energy corresponding to the excitation in its π3(Y) state. It can be emphasized that the formation of the iminium from the (Gly)$_3$-Tyr$^+$ needs more energy, in relation to the observation on dipeptides. Instead of considering the n(Nt) or π3(Y) states as references, one can take the fundamental π1(Y) state and the energies needed to reach AS1 from π1(Y), denoted ΔE_{AS1}(CF1/π1(Y)), are presented in Table 5. The ΔE_{AS1}(CF1/π1(Y)) for (Gly)$_3$-Tyr$^+$ is larger than that for the two other peptides, as previously noted for the other energies. It is also larger in the case of the CF1c conformation, which is quite normal since this is the lowest energy conformation of the cation.

B. Replacement of One Aliphatic Amino acid by Glycine: The (R2G)-Tyr Isomers, R = A or L. The three isomers Gly-$(X)_2$-Tyr, X-Gly-X-Tyr and $(X)_2$-Gly-Tyr, globally represented by [X_2-Gly]-Tyr, have been studied for X = Ala and Leu. All the starting geometries for the optimizations have been taken from X_3-Tyr, either for the neutral (11 conformations each) or for the cation (3−6 conformations each).

B.1. Relative Energies of the Neutrals and the Cations. From Table 2, the quasi degenerescence of CF1 and CF2 does no

TABLE 5: Energy Differences (eV) between the Asymptote Level AS1 Corresponding to the Iminium Formation and Several References[a]

	$(Gly)_2^+$	$(Ala)_2^+$	$(Leu)_2^+$	Gly-Ala$^+$	Ala-Gly$^+$
ΔE_{diss}(noZPE)	1.40	0.93	0.85	1.46	0.88
ΔE_{diss}(ZPE)	1.48	1.00	0.90	1.53	0.95

	$(Gly)_3$-Tyr$^+$	$(Ala)_3$-Tyr$^+$	$(Leu)_3$-Tyr$^+$
ΔE_{diss}(noZPE)	ND	ND	1.64
ΔE_{diss}(ZPE)	ND	ND	ND
ΔE_{AS1}(CF1,n(Nt))/ΔE_{AS1}(CF1,π3(Y))	−0.42/−1.31	−0.88/−1.96	−0.94/−2.34
ΔE_{AS1}(CF2,n(Nt))/ΔE_{AS1}(CF2,π3(Y))	0.44/−1.71	−0.08/−2.32	0.18/−2.59
ΔE_{AS1}(CF1c,π3(Y))	−0.69	−1.28	−1.50
ΔE_{AS1}(CF1,π1(Y))	2.12	1.46	1.28
ΔE_{AS1}(CF2,π1(Y))	1.73	1.12	0.92
ΔE_{AS1}(CF1c,π1(Y))	3.03	2.46	2.26

[a] The ΔE_{diss}() refer to the optimized geometry of the cation in its n(Nt) state, with or without the zero point energy ZPE correction. The ΔE_{AS1}(CF1,n(Nt))/(ΔE_{AS1}(CF1,π3(Y))) and ΔE_{AS1}(CF2,n(Nt))/(ΔE_{AS1}(CF2,π3(Y))) refer to the energy obtained by adding the ionization energy necessary to form the n(Nt) (π3(Y)) state to the energy of the neutral, either CF1 or CF2. The ΔE_{AS1}(CF1c,π3(Y)) refer to the energy obtained by adding the excitation energy of the π3(Y) state to the energy of the cation in its CF1c geometry. The ΔE_{AS1}(CFx,π1(Y))(x = 1,2,1c) are determined in the same way except that the reference state is π1(Y). Abbreviation: ND = not determined.

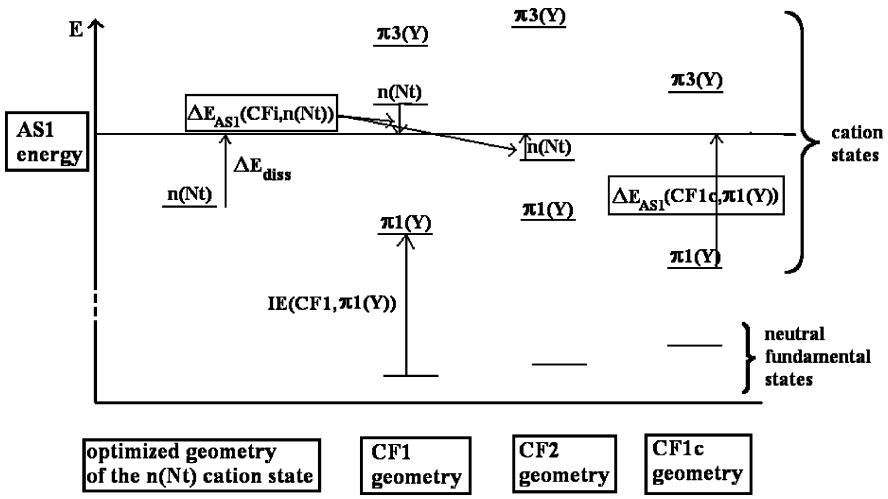

Figure 6. Schematic view of the energy level of the dissociation asymptote AS1 compared to those of some electronic states for different geometries.

longer hold though CF2 remains close in the case of Gly-$(X)_2$-Tyr (around 3.8 kJ/mol). However, the most striking difference is observed for X-Gly-X-Tyr, for which CF2 becomes the lowest energy conformation, CF1 and CF3 being very close to one another. Thus, X-Gly-X-Tyr could show peculiar experimental properties as compared to the other [X_2-Gly]-Tyr peptides.

For the cations, by reference to X_3-Tyr, the same conformation CF1c is found to be the lowest in energy, much below the other ones (from 12 to 25 kJ/mol).

B.2. Ionization Energies. The same general tendencies are found for the [X_2-Gly]-Tyr$^+$ cation electronic states by reference to X_3-Tyr$^+$ ones, as presented in Table 6. The π(3p) and π(2p) states are very close, though somewhat less close in the case of CF1c, and they can even be either degenerate or inverted. The π(1p) state also lies rather near the two others. The relative energy ΔE_{exc} of these states varies in a significant way as a function of the conformation, which is not the case for the π3(Y) the ΔE_{exc} of which lies in the range [3.40−3.80 eV]. The π2(Y) presents an intermediate behavior in that its ΔE_{exc} does not vary much between the neutral conformations, in the [0.8−0.95 eV] range, but it changes significantly for the cation conformation CF1c with a ΔE_{exc} around 1.60 eV. Thus, the relative position of the π2(Y) state as compared to the π(ip) states varies from one conformation to the other. The n(Nt) state is always lower than the π3(Y) one for the neutral conformations but not for CF1c, except in the case of $(Leu)_2$-Gly-Tyr. For this latter peptide at the CF1 geometry, the ionized MO leading to a π3(Y) state is also essentially delocalized on the side chains of the two leucines and contains a very small π3(Y) density; this could produce a much less efficient electronic excitation. Similarly, for that same state of Gly-$(Leu)_2$-Tyr$^+$ and Leu-Gly-Leu-Tyr$^+$ in their CF1 conformation, the π3(Y) density is mixed with either (Sdch(L2) + n(tO═C)) or π(COOH) respectively; n(tO═C) is also part of the ionized MO density leading to the π3(Y) state for CF1 of $(Ala)_2$-Gly-Tyr.

Discussion

From the results, it clearly appears that the conformation has a large influence on the position of the electronic states and this influence is much larger than that of the size of the side chain. In the case of $(Ala)_3$-Tyr and $(Leu)_3$-Tyr, two neutral conformations, CF1 and CF2, are certainly populated, with maybe three for $(Ala)_3$-Tyr. The replacement of one Ala or one Leu by Gly in the tetrapeptides $(Ala)_3$-Tyr and $(Leu)_3$-Tyr lifts the near degeneracy of CF1 and CF2. For two isomers, CF1 was clearly the lowest energy conformation while for X-Gly-X-Tyr, CF2 was found to be the most stable one.

Nevertheless, the qualitative scheme related to the energy levels of the cations was the same for the conformations of these peptides compared to those of $(Ala)_3$-Tyr and $(Leu)_3$-Tyr. Thus, differences observed experimentally between X_3-Tyr and its [X_2-Gly]-Tyr substituted isomers should be related to the

TABLE 6: Ionization Energies (IE) and Cation Excitation Energies (ΔE_{exc}) Calculated at the OVGF/6-31G Level for Three Conformations of the Three Isomers of [$(Ala)_2$-Gly]-Tyr and [$(Leu)_2$-Gly]-Tyr

CF1		CF2		CF1c	
MO description	IE (eV)/ΔE_{exc}	MO description	IE (eV)/ΔE_{exc}	MO description	IE (eV)/ΔE_{exc}
		Gly-$(Ala)_2$-Tyr			
π1(Y)	7.77/0.0	π1(Y)	8.04/0.0	π1(Y)	5.97/0.0
π2(Y)	8.69/0.92	π(3p)	8.62/0.58	π2(Y)	7.56/1.59
π(3p)	8.73/0.96	π(2p) + n_O(3p) + π(3p)	8.63/0.59	π(3p)	8.69/2.72
π(2p) + n_O(3p)	8.87/1.10	π2(Y)	8.86/0.82	π(2p) + n_O(3p)	8.98/3.01
π(1p) + n_O(2p)	9.28/1.51	π(1p) + n_O(2p)	9.00/0.96	π(1p) + n_O(2p)	9.22/3.25
n(Nt) + n_O(1p)	10.21/2.44	n(Nt) + n_O(1p)	9.42/1.38	σ's(Y) + n_O(1p)	9.55/3.58
n_O(3p) + π(2p)	10.27/2.50	n_O(3p) + π(2p)	10.04/2.00	π3(Y)	9.76/3.79
n_O(2p) + π(1p)	10.58/2.81	n_O(2p) + π(1p)	10.26/2.22	n_O(3p) + π(2p)	9.92/3.95
n(tO═C)	10.72/2.95	n_O(1p) + n(Nt)	10.65/2.61	n(Nt) + n_O(1p)	10.33/4.36
n(Nt) + n(tO═C) + n_O(1p)	11.12/3.35	n(tO═C)[+n_O(3p)]	10.94/2.90	n_O(2p) + π(1p)	10.60/4.63
π3(Y)	11.18/3.41	π(COOH)	11.53/3.49	n(tO═C)	10.79/4.82
π(COOH) + σ's(Y)	11.45/3.68	π3(Y)	11.54/3.50	σ's(Y-sdY) + n(tO═C) + n(Nt)	11.12/5.15
σ's(Y) + π(COOH)	11.60/3.83	σ's(Y)	11.84/3.80	σ's(Y-sdY) + n(tO═C) + n(Nt)	11.15/5.18
		Ala-Gly-Ala-Tyr			
π1(Y)	7.75/0.0	π1(Y)	8.08/0.0	π1(Y)	5.98/0.0
π(3p)	8.61/0.86	π(3p)	8.64/0.56	π2(Y)	7.57/1.59
π2(Y)	8.66/0.91	π(2p) + n_O(3p)	8.66/0.58	π(3p)	8.69/2.71
π(2p) + n_O(3p)	8.84/1.09	π2(Y)	8.91/0.83	π(2p) + n_O(3p)	9.00/3.02
π(1p) + n_O(2p)	9.33/1.58	π(1p) + n_O(2p)	9.06/0.98	π(1p) + n_O(2p)	9.29/3.31
n(Nt) + n_O(1p)	10.14/2.39	n(Nt) + n_O(1p)	9.31/1.23	σ's(Y) + n_O(1p)	9.57/3.59
n_O(3p) + π(2p)	10.17/2.42	n_O(3p) + π(2p)	10.11/2.03	π3(Y)	9.76/3.78
n_O(2p) + π(1p)	10.58/2.83	n_O(2p) + n_O(1p) + n(Nt)	10.39/2.31	n_O(3p) + π(2p)	9.93/3.95
n(tO═C) + n_O(1p)	10.67/2.92	n_O(1p) + n(Nt) + n_O(2p)	10.63/2.55	n(Nt) + n_O(1p)	10.21/4.23
π(COOH)	11.12/3.37	n_O(COOH) [+n_O(3p)]	10.93/2.85	n(tO═C) + n_O(2p) + π(1p)	10.74/4.76
π3(Y) [+π(COOH)]	11.20/3.45	π(COOH)	11.49/3.41	n_O(2p) + π(1p) + n(tO═C)	10.71/4.73
n(Nt) + n(tO═C) + n_O(1p)	11.20/3.45	π3(Y)	11.52/3.44	σ's(Y-sdY) [+n(Nt) + n_O(1p) + n(tO═C)]	11.08/5.10
σ's(Y)	11.62/3.87	σ's(Y)	11.86/3.78	σ's(Y-sdY) + n(tO═C)	11.15/5.17
				π(COOH)	11.65/5.67
		$(Ala)_2$-Gly-Tyr			
π1(Y)	7.76/0.0	π1(Y)	8.01/0.0	π1(Y)	6.00/0.0
π2(Y)	8.69/0.93	π(3p)	8.68/0.67	π2(Y)	7.57/1.57
π(3p)	8.80/1.04	π(2p) + n_O(3p)	8.70/0.69	π(3p)	8.74/2.74
π(2p) + n_O(3p)	8.95/1.19	π2(Y)	8.91/0.90	π(2p) + n_O(3p)	9.12/3.12
π(1p) + n_O(2p)	9.30/1.54	π(1p) + n_O(2p)	9.03/1.02	π(1p) + n_O(2p)	9.23/3.23
n(Nt) + n_O(1p)	10.08/2.32	n(Nt) + n_O(1p)	9.30/1.29	σ's(Y) + n_O(1p)	9.53/3.53
n_O(3p) + π(2p)	10.35/2.54	n_O(3p) + π(2p)	10.09/2.08	π3(Y)	9.79/3.79
n_O(2p) + n(Nt) + n_O(1p)	10.65/2.89	n_O(2p) + n_O(1p) + n(Nt)	10.26/2.25	n_O(3p) + n(Nt) + n_O(2p)	10.09/4.09
n(tO═C) + n_O(2p) + n_O(1p)	10.76/3.00	n_O(1p) + n(Nt) + n_O(2p)	10.57/2.56	n(Nt) + n_O(3p) + n_O(1p)	10.17/4.17
n(Nt) + n_O(1p) + n(tO═C)	11.02/3.26	n(tO═C) [+n_O(3p)]	10.93/2.92	n_O(2p) + π(1p)	10.62/4.62
π3(Y) + n(tO═C)	11.18/3.42	π(COOH)	11.49/3.48	n(tO═C)	10.80/4.80
π(COOH) + σ's(Y)	11.43/3.67	π3(Y)	11.52/3.51	σ's(Y) + n(Nt) + n_O(1p)	11.08/5.08
σ's(Y) + π(COOH)	11.61/3.85	σ's(Y)	11.86/3.85	σ's(Y) + n(tO═C)	11.19/5.19
				π(COOH)	11.64/5.64
		Gly-$(Leu)_2$-Tyr			
π1(Y)	7.72/0.0	π1(Y)	8.03/0.0	π1(Y)	6.15/0.0
π2(Y)	8.65/0.93	π(2p) + $n_{O,Np}$(3p)	8.52/0.49	π2(Y)	7.84/1.69
π(3p)	8.70/0.98	π(3p) [+π(2p)]	8.62/0.59	π(3p)	8.52/2.37
π(2p) + n_O(3p)	8.76/1.04	π2(Y)	8.86/0.83	π(2p) + n_O(3p)	8.75/2.60
π(1p) + n_O(2p)	9.16/1.44	π(1p) + n_O(2p)	8.88/0.85	n_O(2p) + π(1p)	9.34/3.19
n(Nt) + n_O(1p)	10.16/2.44	n(Nt) + n_O(1p)	9.38/1.35	σ's(Y) + n_O(1p)	9.71/3.56
n_O(3p) + π(2p)	10.23/2.51	π(2p) + n_O(3p)	9.96/1.93	π3(Y)	9.91/3.76
n_O(2p) + π(1p)	10.52/2.80	n_O(2p) + π(1p)	10.19/2.16	π(2p) + n_O(3p)	10.05/3.90
n(tO═C) [+n_O(1p) + n_O(3p)]	10.76/3.04	Sdch(L3) + n(Nt) + n_O(1p)	10.80/2.77	n(Nt) + n(tO═C)	10.42/4.27
Sdch(L3)	11.22/3.50	Sdch(L3) + n(Nt) + n_O(1p)	10.87/2.84	n(Nt) + n(tO═C)	10.59/4.44
Sdch(L3) + Sdch(L2) + n(Nt)	11.23/3.51	Sdch(L3)	10.98/2.95	π(1p) + n_O(2p)	10.73/4.58
Sdch(L3)	11.24/3.52	Sdch(L3)	11.05/3.02		
π3(Y) + Sdch(L2) + n(tO═C)	11.36/3.64	n(tO═C)	11.07/3.04		
Sdch(L2) + n(Nt) + π(COOH)	11.39/3.67	Sdch(L2)	11.51/3.48		
Sdch(L3) + Sdch(L2)	11.45/3.73	Sdch(L2)	11.53/3.50		
Sdch(L2)	11.47/3.75	π3(Y)	11.53/3.50		
		π(COOH)	11.55/3.52		
		Sdch(L2)	11.64/3.61		

TABLE 6 (Continued)

CF1		CF2		CF1c	
MO description	IE (eV)/ΔE_{exc}	MO description	IE (eV)/ΔE_{exc}	MO description	IE (eV)/ΔE_{exc}
		Leu-Gly-Leu-Tyr			
π1(Y)	7.66/0.0	π1(Y)	8.02/0.0	π1(Y)	6.17/0.0
π(3p)	8.56/0.90	π(3p) + π(2p)	8.59/0.57	π2(Y)	7.85/1.68
π2(Y)	8.59/0.93	π(3p) + π(2p)	8.65/0.63	π(3p)	8.53/2.36
π(2p) + n_O(3p)	8.75/1.09	π2(Y)	8.86/0.84	π(2p) + n_O(3p)	8.78/2.61
π(1p) + n_O(2p)	9.26/1.60	π(1p) + n_O(2p)	9.02/1.00	n_O(2p) + π(1p)	9.46/3.29
n(Nt) + n_O(1p)	9.94/2.28	n(Nt) + n_O(1p)	9.19/1.17	σ's(Y) + n_O(1p)	9.67/3.50
n_O(3p) + π(2p)	10.13/2.47	π(2p) + n_O(3p)	10.06/2.04	π3(Y)	9.91/3.74
n_O(2p) + π(1p)	10.50/2.84	π(1p) + n_O(2p) + n(Nt)	10.33/2.31	π(2p) + n_O(3p)	10.07/3.90
n(tO═C) [+n_O(1p) + n_O(3p)]	10.65/2.99	Sdch(L3)	10.85/2.83	n(Nt) + n_O(1−3p) + n(tO═C) + σ's(Y), deloc	10.31/4.14
π(COOH) + Sdch(L3) + π3(Y)	11.12/3.46	Sdch(L3)	10.92/2.90		
n(tO═C) + n(Nt)	11.17/3.51	Sdch(L3)	11.02/3.00	n(tO═C)	10.56/4.39
Sdch(L3)	11.22/3.56	Sdch(L3)	11.09/3.07	π(1p) + n_O(2p), + ..., deloc	10.91/4.74
π3(Y) + π(COOH)	11.24/3.58	n(tO═C) [+n_O(3p) + Sdch(L3)]	11.11/3.09		
Sdch(L3)	11.27/3.61	Sdch(L1)	11.50/3.48		
		π3(Y)	11.52/3.50		
		π(COOH)	11.56/3.54		
		Sdch(L1)	11.59/3.57		
		$(Leu)_2$-Gly-Tyr			
π1(Y	7.73/0.0	π1(Y)	8.03/0.0	π1(Y)	6.16/0.0
π2(Y)	8.66/0.93	π(2p) + n_O(3p)	8.69/0.66	π2(Y)	7.86/1.70
π(3p)	8.81/1.08	π(3p)	8.70/0.67	π(3p)	8.55/2.39
π(2p) + n_O(3p)	8.94/1.21	π2(Y)	8.86/0.83	π(2p) + n_O(3p)	8.88/2.72
π(1p) + n_O(2p)	9.17/1.44	π(1p) + n_O(2p)	8.87/0.84	π(1p) + n_O(2p)	9.39/3.23
n(Nt) + n_O(1p)	9.88/2.15	n(Nt) + n_O(1p)	9.12/1.09	n(Nt) + n_O(1p) + σ's(Y)	9.61/3.45
n_O(3p) + π(2p)	10.34/2.61	n_O(3p) + π(2p)	10.06/2.03	π3(Y)	9.90/3.74
n_O(1p) + n_O(2p) + n(Nt)	10.54/2.81	n_O(2p) + π(1p)	10.20/2.17	n(Nt) + π(2p) + n_O(3p)	10.15/3.99
n_O(2p) + n_O(1p) + n(Nt) + n(tO═C)	10.75/3.02	n_O(1p) + n(Nt)	10.47/2.44	n_O(3p) + π(2p) + n(Nt)	10.27/4.11
n_O(tO═C)	10.90/3.17	n_O(COOH)	10.96/2.93	n_O(COOH)	10.55/4.39
Sdch(L2) + n_O(tO═C)	11.40/3.67	Sdch(L2) + π(COOH)	11.48/3.45	π(1p) + n_O(2p) + Sdch(L2)	10.76/4.60
Sdch(L1) + Sdch(L2) [+π3(Y)]	11.42/3.69	Sdch(L2)	11.50/3.47		
π(COOH) + Sdch(L1)	11.55/3.82	π3(Y)	11.51/3.48		
Sdch(L1)	11.58/3.85	Sdch(L2) + Sdch(L1)	11.53/3.50		
Sdch(L1)	11.58/3.85	π(COOH) + Sdch(L1)	11.55/3.52		
Sdch(L2)	11.58/3.85	Sdch(L1)	11.57/3.54		
Sdch(L2)	11.64/3.91	Sdch(L2)	11.64/3.61		
Sdch(L1) + σ's(Y)	11.75/4.02	Sdch(L1)	11.69/3.66		

conformation preference of the [X_2-Gly]-Tyr rather than the energetic framework in the cation. However, it must be stressed that the determination of the coupling elements between the states play a leading role in the CT process and these elements are very dependent on the conformation. This point was already emphasized in the literature in the case of neutral peptide excitation.[40−42]

One peculiar feature about the $(Leu)_2$-Gly-Tyr^+ cation is that, in the CF1 conformation, it seems hardly excitable to a π3(Y) state according to the MOs description. As a matter of fact, the π3(Y) density contributes very little to the twelfth state density at 11.42 eV. The question of the cation excitation efficiency is thus to be pointed out for this peptide.

By taking into account only the excess energy available for dissociation from the n(Nt) state or the π3(Y) state, the iminium cation $[NH_2{=}CHR]^+$ should be obtained for all the peptides except those for which the cation is formed in the CF2 conformation, i.e., X-Gly-X-Tyr peptides and part of the $(Ala)_3$-Tyr and $(Leu)_3$-Tyr populations. Though the relative energies for the dissociation asymptotes obtained for the $(Ala)_2^+$ dipeptide cation would probably be different in the tetrapepdides due to the influence of the conformation, it is reasonable to extrapolate that the dissociation asymptote leading to the formation of the COOH radical and the iminium $[X{-}X'{-}NH{=}CHR]^+$ cation (AS3 higher than AS1 by 0.56 eV in $(Ala)_2^+$) could be reached by the cation in its CF1 or CF1c geometry, either from the n(Nt) state or from the π3(Y) state. The fact that no such cation is observed in the mass spectra and that nearly only the terminus iminium cation appears is again linked to the great efficiency of the CT process, i.e., to the electronic coupling between the states leading from the initial π3(Y) state to the final n(Nt) one. It has to be emphasized that the passage of the charge from the tyrosine to the NH_2 terminus, i.e., the change from the π3(Y) to the n(Nt) state, could happen by a direct electronic coupling between the two states. As a matter of fact, for the cation in its CF1 conformation, the π3(Y) state is very near a second n(Nt)-type state for all the tetrapeptides except $(Leu)_2$-Gly-Tyr for which the second n(Nt) state is much lower in energy than the twelfth state containing a small π3(Y) density. The case of $(Ala)_3$-Tyr is even more striking since the π3(Y) state is itself delocalized on the NH_2 terminus which means that the charge is already of the NH_2 terminus as soon as the π3(Y) state is formed.

The following discussion will be made essentially be reference to the one-color and two-color experiments by Weinkauf et al.[6−8] and Cui et al.[10] In the one-color experiment of Weinkauf et al., the ionization to the π1(Y) state is immediately followed by the excitation to the π3(Y) state by absorption of 3 photons of UV radiation in the 4.4−4.8 eV range, while in the two-color experiment, the ionization to the π1(Y) state is followed

by the population of an excited state with a 2.2−2.4 eV visible (vis) radiation eventually followed by another photon absorption of the same vis radiation to reach the $\pi 3$(Y) state with enough energy to dissociate. In the case where CT occurs between the two VIS photons absorption, this cation $\pi 3$(Y) state is no longer reachable since the chromophore is no longer charged. With the first 2.2−2.4 eV of energy absorbed, there is not enough excess energy to lead to dissociation in the time scale of the experiment.

Let us start the ionization and excitation processes from the CF1 geometry, which is supposed to be the most stable neutral conformer except for Ala-Gly-Ala-Tyr and Leu-Gly-Leu-Tyr. With the one-color experiment, many states can be populated from the initial $\pi 3$(Y) state with the very close second n(Nt) state for nearly all peptide cations. Thus, the observation of selective dissociation at the NH_2 terminus cannot be explained on the basis of the energy position of the bridge states compared with that of the NH_2 terminus. This should rather be a matter of coupling efficiency between the $\pi 3$(Y) state and the n(Nt) ones. Generally speaking, this efficiency is larger when the energy difference between the states is and remains small,[43] but the energy difference is not the only parameter entering the equation, the shape of the potential energy surfaces as well as the nuclei velocities playing a role as well. With the two-color experiment, at 2.2−2.4 eV, one can reach all the π(ip) states as well as the n(Nt) one, and from the results ΔE(CFx,$\pi 1$(Y)) in Table 5, there is enough energy to lead to dissociation in all the cases. Furthermore, this energy range corresponds very precisely to the energy of the n(Nt) state. Thus, if the photoabsorption is efficient enough, the reorganization of the electronic density from $\pi 1$(Y) to n(Nt) occurs as if a CT has happened leading to a neutralized chromophore that can no longer absorb. From the results in Table 5, the minimum energy needed to reach AS1 is on the order of 1.3−1.5 eV except for $(Gly)_3$-Tyr^+ where it grows up to 2.12 eV. These values correspond to the threshold for slow dissociation observed by Cui et al. in their one-color experiment (266 nm). In this case, the CT until the NH_2 terminus has to imply conformation changes as proposed by Schlag et al.[5] in their bifunctional model since the n(Nt) state is no longer reachable at this CF1 conformation and at this low energy.

Instead of considering the CF1 geometry, one can imagine ionization and excitation from CF2. As for CF1, there are many possible states under $\pi 3$(Y) that can be reached, and thus CT is also possible in principle, the n(Nt) final state being even lower than that in CF1. However, one cannot find a n(Nt)-like state very close to the $\pi 3$(Y); they are always significantly lower in energy (0.7−1.2 eV), which probably compromises the efficiency of the direct coupling between these states. As to the slow dissociation, the necessary energy is even lower than in the case of CF1 (see Table 5), significantly lower than the experimental threshold observed by Cui et al.

What happens if the ionized peptide in its $\pi 1$(Y) state has time to relax to its optimal geometry, i.e., if the excitation after the ionization starts from CF1c? The 4.4−4.8 eV excitation (one-color experiment) is able to produce the n(Nt) state since this is the energy range corresponding to this state. As to the 2.2−2.4 eV excitation, it could produce a direct CT to the π(3p) state only but it has about the same energy as the AS1 asymptote, except for $(Gly)_3$-Tyr^+, and could lead to slow dissociation as observed by Cui et al. in their two-color experiments (266 + 579 nm), where the cations are certainly in their optimized geometries since a relaxation time of 1980 ms follows the ionization.

To the suggestion of Weinkauf et al. stating that each amino acid in zero-order contributes semi-independently to the potential energy surface (PES) of the whole polypeptide, we can answer that this is not true. First, from a previous study on amino acids ionization energies,[20] it is not possible to attribute an IE to either a n(N) or a n(O) of Gly, Ala or Leu because the states are delocalized on both pairs (n(N) ± n(O)). Nevertheless, if one considers the two delocalized states (n(N) ± n(O)) and their related IE, the energy intervals go from 9.8−10 and 11.20−11.30 for Gly to 9.50−9.70 and 10.80−11.00 for Leu. Second, if one considers the IE of the $\pi(i\text{p})$, they all are lower than the first interval and furthermore, they are different for each $\pi(i\text{p})$ and depends on the conformation. Thus, the amino acids have clearly lost their individuality in the polypeptide chain.

Conclusion

The large influence of the conformation on the position of the cation energy levels was pointed out. The same lowest energy conformation of the neutral (CF1) or the cation (CF1c) is found for all the tetrapeptides except for the X-Gly-X-Tyr (CF2). Two conformations of the neutral should be observed experimentally for $(Ala)_3$-Tyr and $(Leu)_3$-Tyr since they are very close in energy.

According to the energy levels in the cation in the two lowest energy conformations of the neutral, the n(Nt) state is reachable with a zero energy barrier from the $\pi 3$(Y) initial excited state. This is not the case in the optimized geometry of the cation CF1c where the n(Nt) state is higher than the $\pi 3$(Y) one, except for $(Leu)_3$-Tyr^+ and $(Leu)_2$-Gly-Tyr^+. Nevertheless, at the absorption energy used in the experiments (4.4−4.8 eV), the n(Nt) state can be formed is the absorption efficiency is high enough. For the peculiar case of $(Leu)_2$-Gly-Tyr^+ in its CF1 conformation, on the basis of the ionized MOs description, it might be that a $\pi 3$(Y) state could not be formed.

The question of the efficiency of the CT has not been addressed in this work since no electronic coupling between the states has been calculated. Nevertheless, on the basis of the large variation of the relative energy position of the states and of the characteristics of the ionized MOs, it could be stressed that it is this parameter that should most vary from one tetrapeptide to the other and from one conformation to the other. In particular, our hypothesis is that the direct coupling between the $\pi 3$(Y) and the n(Nt) state in the CF1 conformation is the major factor of the high efficiency and selectivity of the CT.

Once the n(Nt) state is formed after the CT, the dissociation leading to the terminus iminium ion $[NH_2{=}CHR]^+$ is easy if the excess energy coming from the formation of the $\pi 3$(Y) state is conserved when the system has passed to the n(Nt) state. Nevertheless, slow dissociation is energetically possible within a range of only 1.3−1.5 eV for the CF1 conformation and 2.4−2.8 eV for the CF1c conformation but the necessary previous CT would only be possible, at these energies, if the conformation changes, as proposed by Schlag et al. in their bifunctional model.

Finally, from the variation of the energies of the $\pi(i\text{p})$ states, it is clear that the amino acids have lost their individuality since no amino acid ionization energy can be found in the polypeptides, in contradistinction to the hypothesis proposed by Weinkauf et al.

Acknowledgment. Georges Dive is chercheur qualifié of the Fonds National de la Recherche Scientifique (FNRS), Brussels.This work was supported by the Belgian program on Interuniversity Poles of Attraction initiated by the Belgian State, Prime Minister's Office, Service fédéraux des affaires scientifiques, techniques et culturelles (PAI no P5/33).

References and Notes

(1) Baranov, L. Ya.; Schlag, E. W. *Z. Naturforsch.* **1999**, *54 a*, 387.

(2) Schlag, E. W.; Sheu, Sheh-Yi; Yang, Dah-Yen; Selzle, H. L.; Lin, S. H. *J. Phys. Chem. B* **2000**, *104*, 7790.

(3) Sheu, Sheh-Yi; Schlag, E. W. *Int. J. Mass Spectrom.* **2002**, *219*, 73.

(4) Sheu, Sheh-Yi; Yang, Dah-Yen; Selzle, H. L.; Schlag, E. W. *J. Phys. Chem. A* **2002**, *106*, 9390.

(5) Schlag, E. W.; Sheu, Sheh-Yi; Yang, Dah-Yen; Selzle, H. L.; Lin, S. H. *Proc. Natl. Acad. Sci. U.S.A.* **2000**, *97*, 1068.

(6) Weinkauf, R.; Schanen, P.; Yang, D.; Soukara, S.; Schlag, E. W. *J. Phys. Chem.* **1995**, *99*, 11255.

(7) Weinkauf, R.; Schanen, P.; Metsala, A.; Schlag, E. W.; Bürgle, M.; Kessler, H. *J. Phys. Chem.* **1996**, *100*, 18567.

(8) Weinkauf, R.; Schlag, E. W.; Martinez, T. J.; Levine, R. D. *J. Phys. Chem. A* **1997**, *101*, 7702.

(9) Schlag, E. W.; Yang, Dah-Yen; Sheu, Sheh-Li; Selzle, H. L.; Lin, S. H.; Rentzepis, P. M. *Proc. Natl. Acad. Sci. U.S.A.* **2000**, *97*, 9849.

(10) Cui, W.; Hu, Y.; Lifshitz, C. *Eur. Phys. J. D* **2002**, *20*, 565.

(11) Hartree, D. R. *Proc. Camb. Philos. Soc. Math. Phys. Sci.* **1928**, *24*, 89.

(12) Fock, V. A. *Z. Phys.* **1930**, *61*, 126.

(13) Szabo, A.; Ostlund, N. S. *Modern Quantum Chemistry. Introduction to Advanced Electronic Structure Theory*; Dover Publications: New York, 1996.

(14) Cederbaum, L. S. *Theor. Chim. Acta* **1973**, *31*, 239.

(15) Cederbaum, L. S.; Domcke, W.; Von Niessen, W. *Chem. Phys.* **1975**, *10*, 459.

(16) Von Niessen, W.; Schirmer, J.; Cederbaum, L. S. *Comput. Phys. Rep.* **1984**, *1*, 57.

(17) Lemierre, V.; Chrostowska, A.; Dargelos, A.; Chermette, H. *J. Phys. Chem. A* **2005**, *109*, 8348.

(18) Markmann, A.; Worth, G. A.; Cederbaum, L. S. *J. Chem. Phys.* **2005**, *122*, 144320.

(19) Deleuze, M. S. *J. Phys. Chem. A* **2004**, *108*, 9244.

(20) Dehareng, D.; Dive, G. *Int. J. Mol. Sci.* **2004**, *5*, 301.

(21) Frisch, M. J.; Trucks, G. W.; Schlegel, H. B.; Scuseria, G. E.; Robb, M. A.; Cheeseman, J. R.; Zakrzewski, V. G.; Montgomery, J. A., Jr.; Stratmann, R. E.; Burant, J. C.; Dapprich, S.; Millam, J. M.; Daniels, A. D.; Kudin, K. N.; Strain, M. C.; Farkas, O.; Tomasi, J.; Barone, V.; Cossi, M.; Cammi, R.; Mennucci, B.; Pomelli, C.; Adamo, C.; Clifford, S.; Ochterski, J.; Petersson, G. A.; Ayala, P. Y.; Cui, Q.; Morokuma, K.; Malick, D. K.; Rabuck, A. D.; Raghavachari, K.; Foresman, J. B.; Cioslowski, J.; Ortiz, J. V.; Baboul, A. G.; Stefanov, B. B.; Liu, G.; Liashenko, A.; Piskorz, P.; Komaromi, I.; Gomperts, R.; Martin, R. L.; Fox, D. J.; Keith, T.; Al-Laham, M. A.; Peng, C. Y.; Nanayakkara, A.; Gonzalez, C.; Challacombe, M.; Gill, P. M. W.; Johnson, B.; Chen, W.; Wong, M. W.; Andres, J. L.; Gonzalez, C.; Head-Gordon, M.; Replogle, E. S.; Pople, J. A. *Gaussian 98*, Revision A.7; Gaussian, Inc.: Pittsburgh, PA, 1998 (www.Gaussian.com).

(22) Parr, R. G.; Yang, W. *Density functional theory of atoms and molecules*; Oxford University Press: New York, 1989.

(23) Kohn, W.; Sham, L. J. *Phys. Rev. A* **1965**, *140*, 1133.

(24) Becke, A. D. *J. Chem. Phys.* **1993**, *98*, 5648.

(25) Hehre, W. J.; Ditchfield, R.; Pople, J. A. *J. Chem. Phys.* **1972**, *56*, 2257.

(26) Frisch, M. J.; Pople, J. A.; Binkley, J. S. *J. Chem. Phys.* **1984**, *80*, 3265.

(27) Abo-Riziq, A. G.; Crews, B.; Bushnell, J. E.; Callahan, M. P.; De Vries, M. S. *Mol. Phys.* **2005**, *103*, 1491.

(28) Huenig, I.; Kleinermanns, L. *Phys. Chem. Chem. Phys.* **2004**, *6*, 2650.

(29) Reha, D.; Valdes, H.; Vondrasek, J.; Hobza, P.; Abo-Riziq, A.; Crews, B.; De Vries, M. S. *Chem.—Eur. J.* **2005**, *11*, 6803.

(30) Valdes, H.; Reha, D.; Hobza, P. *J. Phys. Chem. B* **2006**, *110*, 6385.

(31) Furche, F.; Burke, K. *Annu. Rep. Comput. Chem.* **2005**, *1*, 19.

(32) Burke, K.; Werschnik, J.; Gross E. K. U. *J. Chem. Phys.* **2005**, *123*, 062206/1−9.

(33) Moret, M.-E.; Tapavicza, E.; Guidoni, L.; Rohrig, U. F.; Sulpizi, M.; Tavernelli, I.; Rothlisberger, U. *Chimia* **2005**, *59*, 493.

(34) Serrano-Andrés, L.; Merchán, M. *J. Mol. Struct.: THEOCHEM* **2005**, *729*, 99.

(35) Grimme, S.; Parac, M. *ChemPhysChem* **2003**, *4*, 292.

(36) Gaussview 2.3, copyright of Semichem Inc. 2003, distributed by Gaussian Inc. (www.Gaussian.com).

(37) Kapota, C.; Ohanessian, G. *Phys. Chem. Chem. Phys.* **2005**, *7*, 3744.

(38) Cable, J. R.; Tubergen, M. J.; Levy, D. H. *J. Am. Chem. Soc.* **1988**, *110*, 7349.

(39) Bakker, J. M.; Plützer, C.; Hünig, I.; Häber, T.; Compagnon, I.; von Helden, G.; Meijer, G.; Kleinermanns, K. *Chem. Phys. Chem.* **2005**, *6*, 120.

(40) Hellings, M.; De Meyer, M.; Verheyden, S.; Hao, Q.; Van Damme, E. J. M.; Peumans, W. J.; Engelborghs, Y. *Biophys. J.* **2003**, *85*, 1894.

(41) Shin, Y. G.; Newton, M. D.; Isied, S. S. *J. Am. Chem. Soc.* **2003**, *125*, 3722.

(42) Pan, C.-P.; Barkley, M. D. *Biophys. J.* **2004**, *86*, 3828.

(43) Desouter-Lecomte, M.; Dehareng, D.; Leyh-Nihant, B.; Praet, M.-Th.; Lorquet, A. J.; Lorquet, J.-C. *J. Phys. Chem.* **1985**, *89*, 214.